Solar Batteries

Deutsche Ausgabe: DOI: 10.1002/ange.201606986
Internationale Ausgabe: DOI: 10.1002/anie.201606986

Integrated Photoelectrochemical Solar Energy Conversion and Organic Redox Flow Battery Devices

*Wenjie Li, Hui-Chun Fu, Linsen Li, Miguel Cabán-Acevedo, Jr-Hau He, and Song Jin**

Abstract: *Building on regenerative photoelectrochemical solar cells and emerging electrochemical redox flow batteries (RFBs), more efficient, scalable, compact, and cost-effective hybrid energy conversion and storage devices could be realized. An integrated photoelectrochemical solar energy conversion and electrochemical storage device is developed by integrating regenerative silicon solar cells and 9,10-anthraquinone-2,7-disulfonic acid (AQDS)/1,2-benzoquinone-3,5-disulfonic acid (BQDS) RFBs. The device can be directly charged by solar light without external bias, and discharged like normal RFBs with an energy storage density of 1.15 Wh L^{-1} and a solar-to-output electricity efficiency (SOEE) of 1.7% over many cycles. The concept exploits a previously undeveloped design connecting two major energy technologies and promises a general approach for storing solar energy electrochemically with high theoretical storage capacity and efficiency.*

Renewable energy technologies generally rely on harvesting energy from our most readily exploitable and only truly limitless source: the sun. With the development over several decades, photovoltaic (PV) solar cells convert solar energy to electricity with increasing efficiency and decreasing cost.[1] However, the intermittent nature of sunlight necessitates the storage of the photogenerated electricity; therefore, further large-scale deployment of solar cells also depends on scalable and inexpensive grid-level energy storage solutions.[2] These would demand new grid-level electrochemical energy storage solutions, such as redox-flow batteries (RFBs).[3] The use of liquid electrolytes in RFBs allows a convenient and low-cost scale up of the energy storage capacity without larger cells, such as the case for lithium-ion batteries; instead, scaling up the energy capacity only entails increasing the amount of redox active species in storage tanks without scaling up the power generation components. Another potential solution would be to directly store solar energy in the chemical bonds of molecular fuels (such as hydrogen gas or hydrocarbons)[4] that could be stored, transported, combusted, or ultimately consumed on demand using a fuel cell device to generate electricity. Despite the intense studies since the 1970s,[5] photoelectrochemical (PEC) solar fuel devices have not become commercially viable so far, which is at least partially due to the kinetic barriers (that is, large overpotentials) for generating chemical fuels from photoexcited carriers at the semiconductor–liquid interface, for example, the hydrogen evolution reaction (HER)[6] and oxygen evolution reaction (OER)[7] for the case of PEC water splitting, that limit the efficiency of such devices.[4a] In contrast, many other redox reactions have facile kinetics (small overpotentials) on the surface of common semiconductors and inert electrodes, which facilitates the collection of the photogenerated carriers from semiconductors and leads to efficient "regenerative" PEC solar cells.[8]

Moreover, the liquid electrolytes containing redox couples utilized in regenerative PEC solar cells are also exactly what are needed for energy storage in RFBs.[3] In RFBs, the electrons (or holes) can be stored in redox couples in aqueous (or non-aqueous) solutions as chemical energy. Specifically, the recently demonstrated RFBs with quinone-based redox couples[9] are particularly attractive for coupling with PEC devices. In these RFBs, both catholyte and anolyte are aqueous electrolytes that contain non-metal organic redox species, thus reducing the material cost ($30–40 per kWh) compared with the more developed vanadium RFBs ($81 per kWh).[9] These RFBs can also have a relatively high energy density exceeding 50 Wh L^{-1}, owing to the high aqueous solubility (>1M) of functionalized quinones. Moreover, quinone-based redox couples such as AQDS and BQDS undergo rapid and reversible electron transfer on many electrodes (such as carbon) without any special catalysts.[9b] The fast kinetics of these redox couples is a significant advantage over the OER and HER processes in PEC water splitting because it can enable unassisted solar-driven charging with less overpotential penalty as well as higher charge (and discharge) power densities.

We note that there have been preliminary efforts[10] to combine solar energy conversion devices with RFBs. However, when TiO_2 liquid junction solar cells[11] and dye-sensitized solar cells[12] were integrated with RFBs,[13] due to the intrinsic efficiency limits of these solar energy conversion devices, these devices suffered from low photocharging current densities (<1.5 mA cm^{-2}) and low overall efficiencies.[10] Even though using separated charging/discharging flow chambers instead of an integrated device design is an slight improvement from simply connecting a solar PV device with a RFB,[14] the more complicated device design, higher cost, and low discharge capacity would limit its potential for practical applications. We argue that fully integrating highly efficient regenerative solar cells, such as those based on Si and

[*] W. Li, Dr. L. Li, Dr. M. Cabán-Acevedo, Prof. S. Jin
Department of Chemistry, University of Wisconsin-Madison
1101 University Avenue, Madison, WI 53706 (USA)
E-mail: jin@chem.wisc.edu
H.-C. Fu, Prof. J.-H. He
Division of Computer, Electrical and Mathematical Sciences and Engineering, King Abdullah University of Science and Technology
Thuwal 23955-6900 (Saudi Arabia)

Supporting information for this article can be found under: http://dx.doi.org/10.1002/anie.201606986.

other mature semiconductors,[1,15] with appropriately potential-matched redox couples that can be used in RFBs in one PEC device will be a more effective strategy. Herein we report an integrated PEC solar energy conversion and electrochemical storage device by integrating silicon solar cells in aqueous electrolytes with RFBs using the same pair of organic quinone based redox couples. We demonstrated that such an integrated PEC-RFB device can be charged under solar illumination without external electric bias and discharged at a current density of 10 mA cm^{-2} with a maximum output voltage of 0.41 V and a discharge capacity of 3.5 Ah L^{-1} over many cycles. This integrated device can utilize solar energy efficiently; an overall direct solar-to-output electricity efficiency (SOEE) of 1.7% has been achieved without significant performance optimization.

As illustrated in Figure 1a, our general integrated device design consists of four electrodes, namely a photocathode and a photoanode (that can be made of Si semiconductor) and a cathode and an anode made of carbon felt. Quinone-based organic redox couple AQDS is used as the catholyte and BQDS as the anolyte (Figure 1b) for both the RFB and PEC cells. In such an integrated PEC-RFB device, solar energy is absorbed by semiconductor electrodes and photoexcited carriers are collected at the semiconductor–liquid electrolyte interface and used to convert the redox couples in the RFB to fully charge up the battery (reduce AQDS to AQDSH$_2$ and oxidize BQDSH$_2$ to BQDS). When electricity is needed, the charged up redox couples will be discharged on the surface of carbon felt electrodes as would happen in the discharge of a RFB to generate the electricity. The electrodes are connected differently in energy delivery and storage mode: the cathode and anode are connected with an external load to discharge the RFB, while the photocathode and photoanode are connected to allow solar-driven unassisted battery recharge. The formal potentials (E^0) for AQDS and BQDS redox couples are 0.21 V and 0.89 V, respectively (Figure 1b), and therefore the photovoltage generated at the Si photoelectrode–liquid junctions is high enough (about 0.55 V + 0.55 V)[6a] to drive the battery charge process so that no external electric voltage or energy is needed. A potentiostat is connected between the photocathode and photoanode to monitor the charging current during our test but not needed for actual device cycling operation. Two electrolyte reservoirs are used to store the catholyte and anolyte, which are constantly pumped through the flow cell.

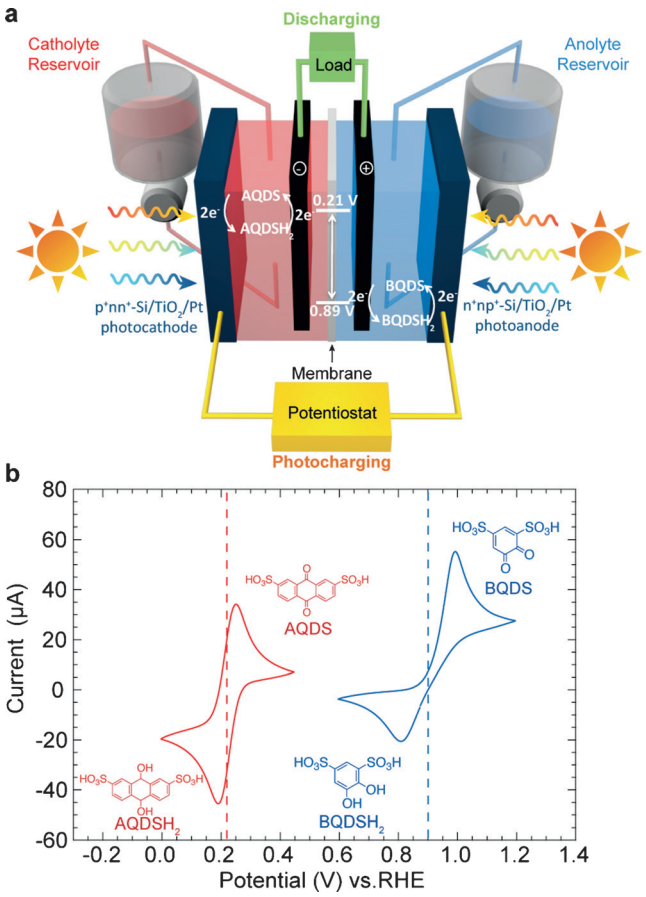

Figure 1. a) The integrated PEC-RFB device using AQDS/BQDS redox couples in catholyte/anolyte. b) Cyclic voltammogram of 5 mM AQDS (red curve) and 5 mM BQDS (blue curve) in 1 M H_2SO_4 scanned at 10 mV s^{-1} on a glassy carbon electrode.

To demonstrate this integrated PEC-RFB device, we first developed and studied the individual components. The RFB was built using aqueous solutions of 0.1 M AQDS and 0.1 M BQDSH$_2$ as catholyte and anolyte, respectively, 1 M sulfuric acid as supporting electrolyte, a Nafion 212 membrane, and two carbon felt electrodes (Supporting Information, Figure S1), similar to a recently reported organic RFB.[9b] Figure 2a shows the representative cycling curves, using

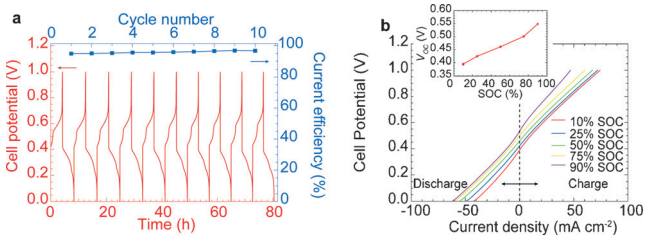

Figure 2. Representative RFB device performance. a) Cell cycling behavior at 10 mA cm^{-2} using 0.1 M AQDS + 1 M H_2SO_4 as catholyte and 0.1 M BQDSH$_2$ + 1 M H_2SO_4 as anolyte. b) Cell potential versus current density at six different SOCs; inset: cell open-circuit potential at different SOCs.

voltage cut-offs of 0 V and 1.0 V, at a constant charging/discharging current of 10 mA cm^{-2}. The RFB has a very stable and reproducible cycling performance with a current efficiency around 96%. Polarization curves and open-circuit potentials (V_{oc}) of the RFB at various states of charge (SOCs) are shown in Figure 2b. The V_{oc} increased from 0.39 V to 0.55 V as the SOC increased from 10% to 90%, which provides an easy way to monitor the SOC of the battery. Considering the possible overpotential caused by diffusion limits and ohmic resistance, this V_{oc} is specifically suitable for being charged by two Si photoelectrodes connected in series, which have a total theoretical voltage of about 1.1 V.[1] We also note that, as shown in previous reports,[16] the chemistry of BQDSH$_2$ is complex and the first charging cycle involved

an "activation reaction" of $BQDSH_2$. Consequently, all the $BQDSH_2$ we used in RFB and PEC characterization was pre-activated in a Teflon H-cell by constant-potential electrolysis.

We then designed silicon photocathodes and photoanodes as regenerative photoelectrodes in AQDS and $BQDSH_2$ aqueous electrolytes, respectively. Because of the dark color of the concentrated AQDS/BQDS solutions, we designed the photoelectrodes to be illuminated from the back side: a p^+nn^+ Si solar cell (called type A) was used as photocathode (Figure 3a) and a n^+np^+ Si solar cell (type B) was used as photoanode (Figure 3c). A key here is to protect silicon from the formation of insulating silicon oxides on the surface, yet preserve the fast kinetics of AQDS and BQDS redox couples. A Ti/TiO_2 (5/40 nm) protection layer was deposited using sputter coating and atomic layer deposition (ALD) on the electrolyte side of the photoelectrodes, followed by a 5 nm layer of sputter-coated Pt to facilitate the charge transfers at the photoelectrode–liquid interface (Figure 3a–c). It is well known that AQDS and BQDS have fast kinetics on glassy carbon,[9b] therefore the Pt layer here was only used for minimizing the charge extraction barrier on the surface of Si, but not a specific catalyst for the AQDS reduction or $BQDSH_2$ oxidation reactions.[17] Other inexpensive but stable metals, such as tungsten and molybdenum, also have the potential to reduce the charge extraction barrier and enable similar PEC performance for these redox reactions (Supporting Information, Figure S2).

We first evaluated the PEC responses of these Ti/TiO_2/Pt coated Si photoelectrodes in 0.1 M AQDS, 0.1 M $BQDSH_2$ as well as in 1 M H_2SO_4 using a three-electrode configuration under simulated one-sun (100 mW cm^{-2}) solar illumination. To determine the equilibrium potential (E_{eq}) of AQDS reduction and $BQDSH_2$ oxidation reaction, linear sweep voltammetry (LSV) scans first were carried out using a 2 cm^2 carbon felt as the working electrode, thus E_{on} as well as the short circuit current density (J_{sc}) of the device can be determined based on E_{eq}. Owing to the existence of the buried pn junction in the Si cells, the E_{on} maintained the same value (0.55 V) for the type A cell in both AQDS solution and H_2SO_4 solution (Figure 3d),[18] while for the type B cell in $BQDSH_2$ solution, the apparent E_{on} was a little lower (Figure 3e), which is perhaps due to the relatively slower diffusion and kinetics of $BQDSH_2$. The overlaid current-density–potential scans (Figure 3f) predict a theoretical maximum operating current density of 16.4 mA cm^{-2} for the integrated PEC-RFB device out of a J_{sc} of 27.4 mA cm^{-2} for photocathode and a J_{sc} of 23.7 mA cm^{-2} for photoanode. The operating current density is mainly limited by the poor fill factors (FF) of the two current PEC cells, especially the type B cell, which may be attributed to the limited surface area of the photoelectrodes and the lower diffusion rate of organic redox couples. To characterize the charging–discharging performance, two potentiostats were used: potentiostat 1 was connected between two photoelectrodes to monitor the photocurrent (blue curve in Figure 4a); potentiostat 2 was connected between two carbon felt electrodes to monitor the potential difference between the two electrodes (red curve). During photocharging, the photoelectrodes were illuminated by an EKE-type illuminator at one sun and no external bias was provided. The V_{oc} of the flow battery increased with time

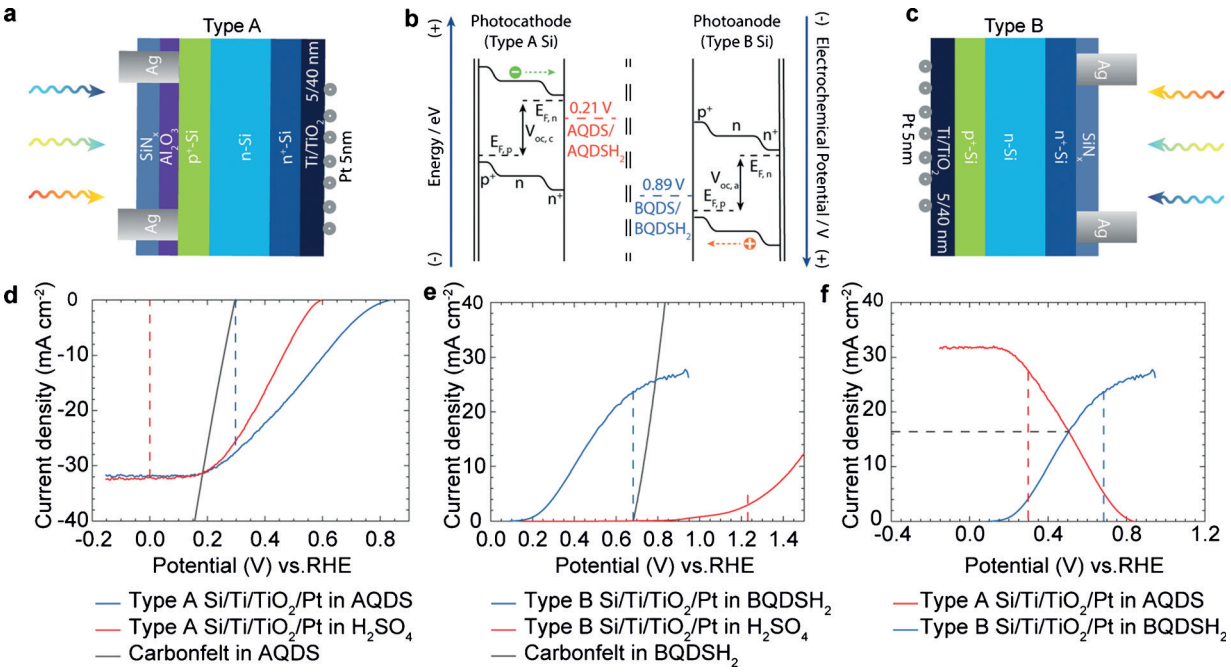

Figure 3. a) Cross-section of type A p^+nn^+-Si/Ti/TiO_2/Pt photocathode; b) band diagram for the photocharging process; c) cross-section of type B n^+np^+-Si/Ti/TiO_2/Pt photoanode. *J–V* data for d) type A p^+nn^+-Si/Ti/TiO_2/Pt electrode measured in 0.1 M AQDS solution or 1 M H_2SO_4 solution; e) type B n^+np^+-Si/Ti/TiO_2/Pt electrode measured in 0.1 M $BQDSH_2$ solution or 1 M H_2SO_4 solution. f) Overlaid *J–V* data for type A p^+nn^+-Si/Ti/TiO_2/Pt electrode measured in 0.1 M AQDS solution with type B n^+np^+-Si/Ti/TiO_2/Pt electrode measured in 0.1 M $BQDSH_2$ solution; the intersection shows the maximum power point.

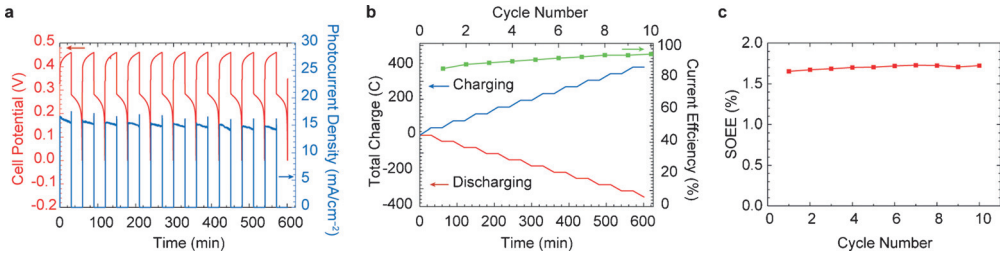

Figure 4. The operation and performance of the integrated PEC-RFB device: a) cell cycling behavior with no bias potential during charging process and a current density of $-10\ mA\,cm^{-2}$ during discharging process; b) total charge and current efficiency of the cell; c) cell SOEE at different cycles.

owing to the increasing SOC. At the same time, the photocurrent decreased slightly because when higher potential was required to charge the battery, lower current could be drawn from the solar cells. During the discharging process, the illumination was turned off and the integrated device was discharged as a normal RFB at a rate of $-10\ mA\,cm^{-2}$ until the cell potential reached 0 V. By integrating the charging/discharging current with respect to time, the charge injected to and drawn from the integrated device as well as the current efficiency can be calculated. The integrated device had a very stable and reproducible cycling performance over ten cycles with a current efficiency around 91% (Figure 4b), which means most of the photoexcited charges can be stored in the aqueous AQDS/BQDS redox couples and redrawn from the integrated device without significant loss caused by side reactions such as HER and OER. Long-term charging/discharging test reveals that the integrated device can be photocharged without external bias to about 80% SOC in 7.3 hours and discharged with a capacity of $3.5\ Ah\,L^{-1}$ (Supporting Information, Figure S3).

To quantitatively evaluate the efficiency of the integrated PEC-RFB device, here we propose a new figure of merit for this type of integrated solar-RFB devices: solar-to-output electricity efficiency (SOEE), which is defined by the ratio of the usable electrical energy delivered by the integrated device ($E_{discharging}$) over the total solar energy input ($E_{illumination}$). The SOEE can be calculated using Equation (1):

$$\mathrm{SOEE}\,(\%) = \frac{E_{discharging}}{E_{illumination}} = \frac{\int I_{out}\,V_{out}\,dt}{\int S\,A\,dt} \qquad (1)$$

where I_{out} is the output (discharging) current, V_{out} is the output voltage, S is the total incident solar irradiance, and A is the total illumination areas of photoanode and photocathode. A typical integrated device showed an average SOEE of around 1.7% over ten cycles (Figure 4c).

The slight photocurrent density decay shown in Figure 4a can be attributed to the photocorrosion of the Si photoelectrodes, which was confirmed by two-electrode PEC measurements of the photoelectrodes before and after cycling test (Supporting Information, Figure S4). The long term stability of the Si photoelectrodes can be further improved by optimizing the protection layer such as increasing the TiO_2 layer thickness and post growth annealing.[17a,19] One of the limitations on the SOEE of the current integrated device is the poor FF of the photoelectrodes, which could be significantly improved by incorporating redox couples that have higher diffusion rates and even faster kinetics, or optimizing the electrolyte flow,[3a] or increasing the surface area of the photoelectrodes by introducing nanostructures on the surface.

Because there have been significant technological developments in regenerative PEC solar cells[15] and RFBs,[3b] we are building on two reasonably mature or rapidly maturing technologies to make a previously unexploited connection to develop a new technology that have a clear pathway for improvement. Fundamentally, the working potential of the integrated device can be further enlarged by replacing redox couples that have higher E^0 in anolyte as well as those with lower E^0 in catholyte, to fully utilize the voltage window of aqueous solution (1.23 V or even higher when considering the overpotentials for HER and OER) and increase device energy density. For example, the recently reported RFB based on 2,6-dihydroxyanthraquinone (2,6-DHAQ) and ferri-ferrocyanide redox couples has a V_{oc} of 1.2 V[20] and is promising for the integrated devices, especially since ferri-ferrocyanide is a very fast redox couple commonly used in PEC cells. Improving the open circuit voltage and the conversion efficiency of regenerative solar cells would further increase the theoretical maximum energy storage density. The single junction crystalline silicon photoelectrodes could be replaced by photoelectrodes that have higher open circuit voltage and higher efficiency, such as GaAs,[21] triple junction amorphous Si,[22] and even potentially high-performance perovskite solar cells.[23] Especially if the formal potentials of the redox couples can be matched well with the band positions of the photocathode and photoanode to create tandem dual-photoelectrode devices similar to tandem dual-photoelectrode PEC water splitting devices,[9] those high voltage photoelectrodes can be even more effectively utilized to drive bias-free charging of the RFBs with higher working voltage, such as the 2,6-DHAQ-ferricyanide RFBs mentioned above, to significantly enhance the energy density. The initial integrated device we demonstrated herein has a promising energy storage density of $1.15\ Wh\,L^{-1}$ at present, but potentially the energy density can reach up to $50\ Wh\,L^{-1}$ [9a,20] and the SOEE can also be significantly increased based on the various improvements discussed above.

In conclusion, we demonstrated a fully integrated photoelectrochemical solar energy conversion and electrochemical storage device by integrating regenerative Si solar cells and all organic AQDS-BQDS RFBs. The use of aqueous electrolytes and non-metal redox couples minimized the prototype device design and fabrication difficulties, thus making the device intrinsically safe, scalable, and cost-effective. The integrated device can be directly charged by solar light without external bias, and discharged like normal RFBs to generate electricity when needed. A promising solar-to-output electricity effi-

ciency of 1.7% and energy storage density of 1.15 $Wh L^{-1}$ have been achieved with the initially demonstrated device without significant optimization, which can be further improved by optimization of devices and operating parameters. Significant enhancement of SOEE and energy storage density can be realized when more suitable redox couples and semiconductors can be designed and paired. This work opens up a new and promising direction for integrating the efficient harvesting and conversion of renewable solar energy and the scalable electrochemical energy storage into a single device, especially for standalone integrated energy systems, allowing for more scalable, efficient, and cost-effective round-trip solar energy utilization.

Acknowledgements

This research is supported by UW-Madison and also partially supported by the NSF Grant DMR-1508558. H.-C.F. and J.-H.H. are supported by the KAUST baseline fund for design and fabrication of Si solar cells.

Keywords: integrated devices · photoelectrochemistry · quinones · redox flow batteries · solar energy conversion

How to cite: *Angew. Chem. Int. Ed.* **2016**, *55*, 13104–13108
Angew. Chem. **2016**, *128*, 13298–13302

[1] M. A. Green, K. Emery, Y. Hishikawa, W. Warta, E. D. Dunlop, *Prog. Photovoltaics* **2016**, *24*, 3–11.
[2] N. S. Lewis, *Science* **2016**, *351*, aad1920.
[3] a) A. Z. Weber, M. M. Mench, J. P. Meyers, P. N. Ross, J. T. Gostick, Q. Liu, *J. Appl. Electrochem.* **2011**, *41*, 1137–1164; b) G. L. Soloveichik, *Chem. Rev.* **2015**, *115*, 11533–11558.
[4] a) M. G. Walter, E. L. Warren, J. R. McKone, S. W. Boettcher, Q. Mi, E. A. Santori, N. S. Lewis, *Chem. Rev.* **2010**, *110*, 6446–6473; b) N. S. Lewis, D. G. Nocera, *Proc. Natl. Acad. Sci. USA* **2006**, *103*, 15729–15735; c) D. G. Nocera, *Acc. Chem. Res.* **2012**, *45*, 767–776.
[5] K. Honda, A. Fujishima, *Nature* **1972**, *238*, 37–38.
[6] a) M. Cabán-Acevedo, M. L. Stone, J. R. Schmidt, J. G. Thomas, Q. Ding, H.-C. Chang, M.-L. Tsai, J.-H. He, S. Jin, *Nat. Mater.* **2015**, *14*, 1245–1251; b) M. Zeng, Y. Li, *J. Mater. Chem. A* **2015**, *3*, 14942–14962; c) M. S. Faber, S. Jin, *Energy Environ. Sci.* **2014**, *7*, 3519–3542.
[7] C. C. L. McCrory, S. Jung, J. C. Peters, T. F. Jaramillo, *J. Am. Chem. Soc.* **2013**, *135*, 16977–16987.
[8] a) J. D. Luttmer, D. Konrad, I. Trachtenberg, *J. Electrochem. Soc.* **1985**, *132*, 1054–1058; b) A. Heller, *Appl. Phys. Lett.* **1981**, *38*, 282–284.
[9] a) B. Huskinson, M. P. Marshak, C. Suh, S. Er, M. R. Gerhardt, C. J. Galvin, X. Chen, A. Aspuru-Guzik, R. G. Gordon, M. J. Aziz, *Nature* **2014**, *505*, 195–198; b) B. Yang, L. Hoober-Burkhardt, F. Wang, G. K. Surya Prakash, S. R. Narayanan, *J. Electrochem. Soc.* **2014**, *161*, A1371–A1380.
[10] M. Yu, W. D. McCulloch, Z. Huang, B. B. Trang, J. Lu, K. Amine, Y. Wu, *J. Mater. Chem. A* **2016**, *4*, 2766–2782.
[11] Z. Wei, D. Liu, C. Hsu, F. Liu, *Electrochem. Commun.* **2014**, *45*, 79–82.
[12] M. Yu, W. D. McCulloch, D. R. Beauchamp, Z. Huang, X. Ren, Y. Wu, *J. Am. Chem. Soc.* **2015**, *137*, 8332–8335.
[13] a) J. Azevedo, T. Seipp, J. Burfeind, C. Sousa, A. Bentien, J. P. Araújo, A. Mendes, *Nano Energy* **2016**, *22*, 396–405; b) N. F. Yan, G. R. Li, X. P. Gao, *J. Mater. Chem. A* **2013**, *1*, 7012–7014.
[14] S. Liao, X. Zong, B. Seger, T. Pedersen, T. Yao, C. Ding, J. Shi, J. Chen, C. Li, *Nat. Commun.* **2016**, *7*, 11474–11478.
[15] P. V. Kamat, K. Tvrdy, D. R. Baker, J. G. Radich, *Chem. Rev.* **2010**, *110*, 6664–6688.
[16] a) Y. Xu, Y.-H. Wen, J. Cheng, G.-P. Cao, Y.-S. Yang, *Electrochim. Acta* **2010**, *55*, 715–720; b) B. Yang, L. Hoober-Burkhardt, S. Krishnamoorthy, A. Murali, G. K. S. Prakash, S. R. Narayanan, *J. Electrochem. Soc.* **2016**, *163*, A1442–A1449.
[17] a) B. Mei, T. Pedersen, P. Malacrida, D. Bae, R. Frydendal, O. Hansen, P. C. K. Vesborg, B. Seger, I. Chorkendorff, *J. Phys. Chem. C* **2015**, *119*, 15019–15027; b) A. G. Scheuermann, J. P. Lawrence, K. W. Kemp, T. Ito, A. Walsh, C. E. D. Chidsey, P. K. Hurley, P. C. McIntyre, *Nat. Mater.* **2016**, *15*, 99–105.
[18] A. J. Bard, A. B. Bocarsly, F. R. F. Fan, E. G. Walton, M. S. Wrighton, *J. Am. Chem. Soc.* **1980**, *102*, 3671–3677.
[19] B. Seger, T. Pedersen, A. B. Laursen, P. C. K. Vesborg, O. Hansen, I. Chorkendorff, *J. Am. Chem. Soc.* **2013**, *135*, 1057–1064.
[20] K. Lin, Q. Chen, M. R. Gerhardt, L. Tong, S. B. Kim, L. Eisenach, A. W. Valle, D. Hardee, R. G. Gordon, M. J. Aziz, M. P. Marshak, *Science* **2015**, *349*, 1529–1532.
[21] B. M. Kayes, H. Nie, R. Twist, S. G. Spruytte, F. Reinhardt, I. C. Kizilyalli, G. S. Higashi, *2011 37th IEEE Photovoltaic Specialists Conference (PVSC)* **2011**, 4–8.
[22] S. Y. Reece, J. A. Hamel, K. Sung, T. D. Jarvi, A. J. Esswein, J. J. H. Pijpers, D. G. Nocera, *Science* **2011**, *334*, 645–648.
[23] a) W. S. Yang, J. H. Noh, N. J. Jeon, Y. C. Kim, S. Ryu, J. Seo, S. Il Seok, *Science* **2015**, *348*, 1234–1237; b) H.-Y. Hsu, L. Ji, H. S. Ahn, J. Zhao, E. T. Yu, A. J. Bard, *J. Am. Chem. Soc.* **2015**, *137*, 14758–14764.

Received: July 19, 2016
Published online: September 21, 2016

